Response to Prof. László Oroszlány

May 29, 2025

1 Question

"The discussion of the properties of Dirac spin liquids plays a central role in the thesis. In electron systems, Dirac cones often appear simultaneously at non-equivalent points in the Brillouin zone. In these systems, scattering between cones can strengthen mechanisms suitable for gap opening. Is there a Dirac spin liquid where Dirac cones are located at different points in the Brillouin zone? In such cases, what phenomena can be attributed to the scattering between cones? Could these processes open a gap in the excitation spectrum of spin liquids?"

I asked Prof. Oroszlány for clarification. He replied: "I was thinking about something like this: for example, in graphene, if we distort the hoppings in a way that corresponds to a Kekulé distortion, then this is equivalent to adding a perturbation to the system that corresponds to the wavevector connecting two Dirac cones. This may open a gap, but not necessarily. My question would be something like this: in similar effective lattice models formulated in terms of Abrikosov fermions, if there are multiple Dirac cones, does this phenomenon also appear?"

Answer

Yes, there are similar phenomena. The nearest neighbor spin 1/2 antiferromagnetic Heisenberg model has a magnetically order ground state with 120° long-range antiferromagnetic order, shown in Fig. 2(a). However, as argued in Refs. [2, 3] using DMRG, introducing second nearest neighbor antiferromagnetic interaction

$$\mathcal{H}^{J_1-J_2} = J_1 \sum_{\langle i,j \rangle} \mathbf{S}_i \cdot \mathbf{S}_j + J_2 \sum_{\langle\langle i,j \rangle\rangle} \mathbf{S}_i \cdot \mathbf{S}_j \tag{1}$$

will favor a magnetically disordered, quantum spin liquid ground state for $J_2/J_1 > 0.06$. As claimed in Refs. [4, 5], the variational ansatz with the lowest variational energy is a Dirac spin liquid with staggered π-0 fluxes in the triangles, so that every unit cell has π fluxes, as shown in Fig. 2(b). This ansatz requires a doubled mean-field unit cell, with two Dirac cones in the mean-field Brillouin zone, connected by the reciprocal lattice vectors at the Γ and M points, as shown in Fig. 2(d).

Remarkably, the nearest neighbor XXZ model

$$\mathcal{H}^{XXZ} = J_\perp \sum_{\langle i,j \rangle} (S_i^x S_j^x + S_i^y S_j^y) + J_z \sum_{\langle i,j \rangle} S_i^z S_j^z - B \sum_i S_i^z \tag{2}$$

has a 120° antiferromagnetically ordered ground state, which has Dirac spin liquid like features (fractionalized gapless excitations), called precursory Dirac spin liquid [6]. This state can be constructed as the Gutzwiller projected ground state of the same staggered $\pi - 0$ flux mean-field ansatz as in the $J_1 - J_2$ model, with the addition of an auxilary external magnetic field creating the 120° antiferromagnetic ordering. The magnetic ordering is shown to open gaps in the Dirac cones.

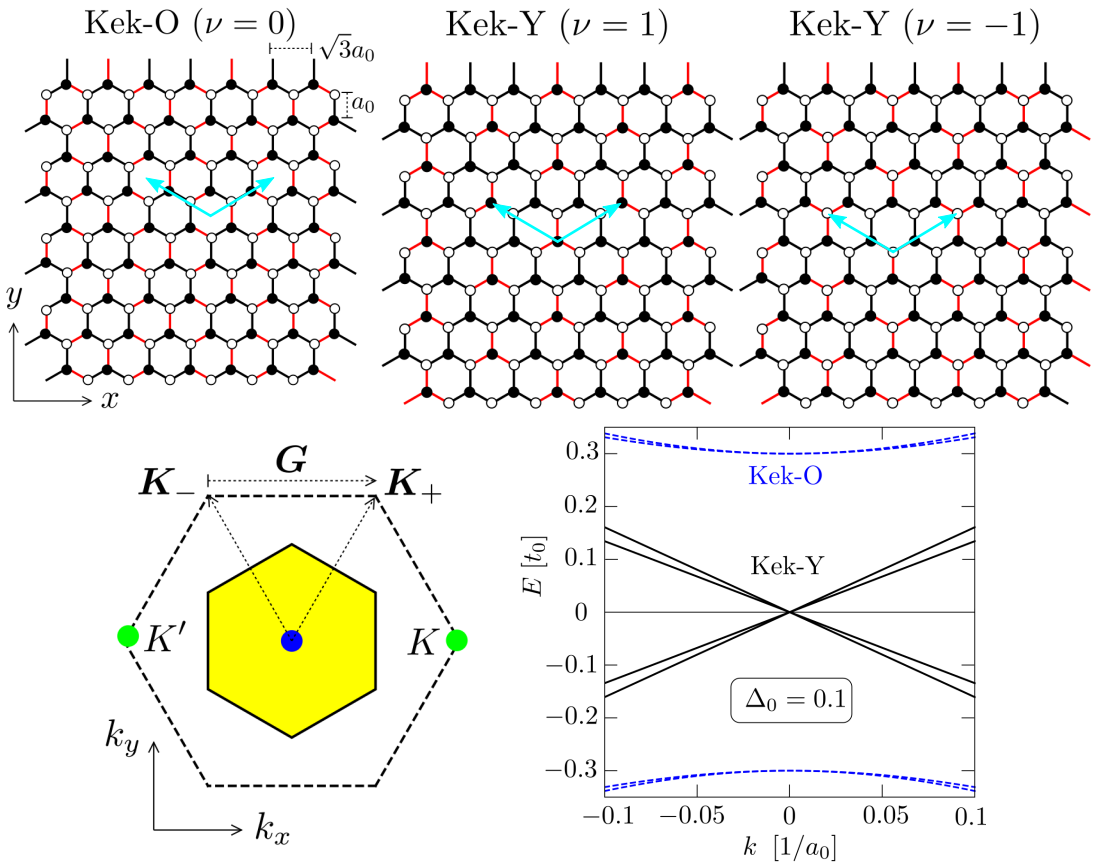

Figure 1: In the first row I show the modulations of the hopping amplitudes corresponding to the Kekulé distortion of the graphene lattice. All these modulations are periodic in the cyan primitive vectors. The reciprocal lattice vectors of the cyan primitive vectors are the $\mathbf{K}_-$ and $\mathbf{K}_+$ vectors shown in the left figure of the second row. The difference $\mathbf{G} = \mathbf{K}_+ - \mathbf{K}_-$ connects the two Dirac cones located at the K points. As shown in the right figure of the second row, the Kek-O modulation opens a gap in the energy spectrum, while the Kek-Y modulations do not. All these figures were taken from Ref. [1] (Figs. [1.] and [2.]).

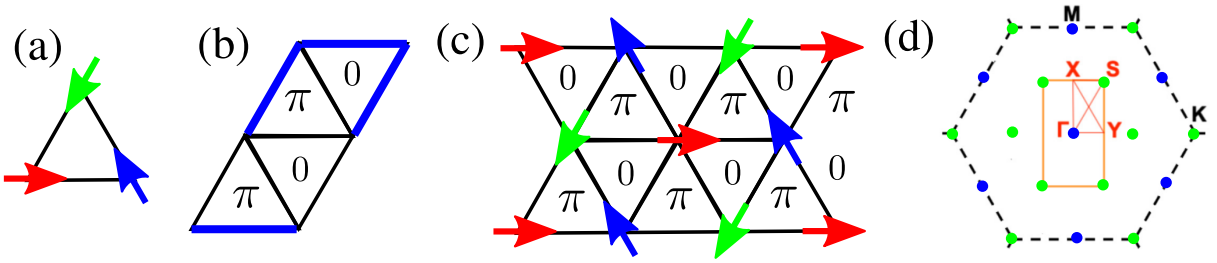

Figure 2: (a) 120° antiferromagnetic ordering, (b) staggered $\pi - 0$ flux ansatz, the blue hoppings are negative, (c) precursory Dirac spin liquid with 120° order, (d) the original, and six times smaller mean-field Brillouin zone, the blue circles are the locations of the Dirac cones for the ansatz shown in panel (b), while the green circles are additional Dirac cones (with small gapes) emerging in the ansatz of panel(c).

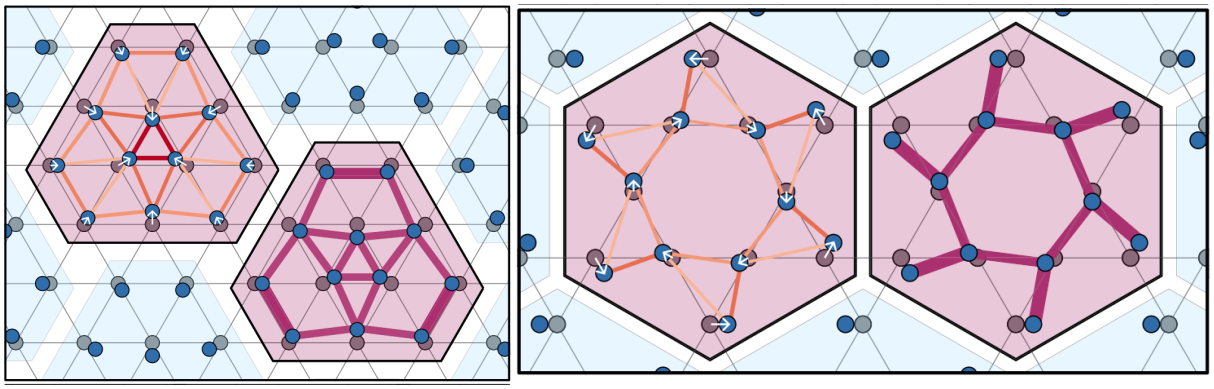

Figure 3: Lattice deformations creating Valence bond solid like patterns, which open gap in the Dirac cones of the Dirac spin liquids on the triangular and kagome lattices. Both figures were taken from Ref. [7] (b and c panels of Fig. 1.).

The 120° order requires a different magnetic unit cell than the doubled unit cell of the staggered $\pi - 0$ flux ansatz. Therefore, to accommodate both the staggered $\pi - 0$ fluxes, and the 120° antiferromagnetic order, the unit cell has to be six times bigger, than the original one, shown in Fig. 2(c). Therefore, the mean-field Brillouin zone is six times smaller than the original one, shown with the orange rectangle in Fig. 2(d). Remarkably, the reciprocal primitive vectors of this mean-field Brillouin zone can connect the Dirac cones at the Γ and M points, which is a similar feature as in the Kek-O perturbation. Moreover, due to the six times smaller mean-field Brillouin zone, the additional Dirac cones with small gapes appear, which were not present without the additional magnetic field.

Another way to open a gap in the Dirac cones of the Dirac spin liquids both on the triangular and on the kagome lattices is via lattice deformations [7] (similar to the Kek-O case), as shown in Fig. 3. Unlike in the previous example, I don't see how the reciprocal vectors characterizing the periodicity of the lattice deformation on the triangular lattice connects the Dirac cones. On the other hand, on the kagome lattice, the lattice deformation is periodic in the same quadrupled unit cell as our Dirac spin liquid ansatz, so the corresponding reciprocal lattice vectors can connect two Dirac cones in neighbouring Brillouin zones.

2 Question

In the case of electron systems, the possible three-dimensional generalizations of Dirac excitations are nodal loop semimetals. In these systems, the zero energy energy excitations are not

isolated points in the Brillouin zone, but continuous nodal lines. Are there higher-dimensional generalizations of the Dirac spin liquids discussed in the thesis, which also have nodal lines?

Answer

Yes, nodal lines appear in the mean-field spectra of the Hamiltonians discussed in Refs. [8, 9, 10] and [11]. In the last one, semimetal and quantum spin liquid phases appear next to each other in the phase diagram, differentiated by the on-site repulsion U of the Hubbard model. For small $U < U_c$ the material is a semimetal, for an intermediate $U_c < U < U_{cm}$ the material is a quantum spin liquid, while for $U_{cm} < U$ there is a transition to an antiferromagnetic phase. The reason why the on-site repulsion changes a semimetal to a quantum spin liquid is that for $U > U_c$ the electronic quasiparticles $c^\dagger_{i,\sigma}$ of the semimetal (carrying both charge and spin 1/2) are fractionalized into spinons $f^\dagger_{i,\sigma}$ (fermionic quasiparticles with spin 1/2 and no charge) and rotons $e^{i\theta_i}$ (bosonic charged quasiparticles with no spin) as $c^\dagger_{i,\sigma} = f^\dagger_{i,\sigma} e^{i\theta_i}$ [12]. The spinons remain gapless and inherits the nodal lines from the nearby semimetallic phase, while the rotons are gapped [11]. This is very similar to the fractionalization in the Abrikosov fermion approach, where we split the spin operators into pairs of *charge neutral* fermionic quasiparticles as $S^a_j = \frac{1}{2}\sum_{\rho,\rho' \in \{\uparrow,\downarrow\}} f^\dagger_{j,\rho} \sigma^a_{\rho,\rho'} f_{j,\rho'}$. In spin models, we don't have rotons, since a spin model emerges in the $U/t \to \infty$ limit, where the charge degrees of freedom are completely frozen.

It is important to note that these nodal lines will appear in the dynamical spin structure factor only if the discussed quantum spin liquid states are stable.

Experimentally, nodal lines were observed in materials having spin liquid ground states in Refs. [13, 14].

3 Question

The author of the dissertation mentions in Sec. 3.1. that he studied the stability of the Dirac spin liquid only against real-valued perturbations, that fit the quadrupled unit cell of the DSL. What methods are available to step out of these constraints, and investigate the effect of more general perturbations?

Answer

Indeed, in my dissertation, I have included only real ansatze in the quadrupled unit cell. However, in our third article about the SU(6) model, my supervisor has studied complex (chiral) ansatze both in the doubled, tripled, and quadrupled unit cells, with a total of π, $2\pi/3$ and $\pi/2$ fluxes in the enlarged unit cells. Furthermore, he also determined the boundary of the ferromagnetic region in the phase diagram, from the gap closing of one- and two-magnon excitations.

Other types of valance bond solid like perturbations can be constructed numerically, using the numerical self-consistent minimization algorithm [15, 16, 17]. In this method, the mean-field approximation is enriched with site-dependent chemical potentials, which are optimized stochastically together with the parameters of the mean-field ansatz, until a convergence of the variational energy is reached. The site-dependent chemical potentials are necessary to reach the uniform occupation of every lattice site on average. Even though this is not as efficient as the Gutzwiller projection, the method can produce valence bond solid like patterns, which can be used to construct Gutzwiller projected variational wavefunctions.

Regarding more general approaches, neural network wavefunctions or tensor network methods as DMRG and PEPS can be used without any assumption of the ground state, but these methods have their own bias, just like variational Monte Carlo methods (e.g. DMRG prefers gapped

ground states). Quantum Monte Carlo methods work very well if there is no sign problem, but even in these cases, they can not calculate the dynamical spin structure factor exactly, because that requires analytical continuation from Matsubara frequencies to real energies, which is not a well-controlled procedure.

4 Question

The first thesis point is about the study of the SU(3) symmetric spin chain. In the $S = 1$ Heisenberg model, the basis of the local Hilbert space is also three-dimensional. What are the similarities and the differences between the $S = 1$, and the SU(3) symmetric models? Are the methods applied in the dissertation also applicable in the case of these lower symmetry models, or is there some qualitative difference between the models that requires fundamentally different methods?

Answer

The methods applied in my thesis are also applicable to any model with lower symmetry, provided that the Hamiltonian in question has a quantum spin liquid ground state.

To see the connection between the spin 1 irreducible representation of SU(2) symmetric models and the fundamental representation of the SU(3) Heisenberg model (both models have three-dimensional local Hilbert spaces on every lattice site), let me consider the SU(2) symmetric bilinear biquadratic model in the $s = 1$ irrep

$$\mathcal{H} = \cos\theta \sum_{i=1}^{N_s} \mathbf{S}_i \cdot \mathbf{S}_{i+1} + \sin\theta \sum_{i=1}^{N_s} (\mathbf{S}_i \cdot \mathbf{S}_{i+1})^2. \tag{3}$$

As discussed in Ref. [18], the model (3) has eight independent local Hermitian operators, three spin vector operators $T^1 = S^x$, $T^2 = S^y$, $T^3 = S^z$, and five quadrupolar operators:

$$T^4 \equiv Q^{xy} = S^x S^y + S^y S^x \tag{4}$$

$$T^5 \equiv Q^{yz} = S^y S^z + S^z S^y \tag{5}$$

$$T^6 \equiv Q^{zx} = S^z S^x + S^x S^z \tag{6}$$

$$T^7 \equiv Q^{x^2-y^2} = (S^x)^2 - (S^y)^2 \tag{7}$$

$$T^8 \equiv Q^{3z^2-r^2} = \frac{1}{\sqrt{3}}[2(S^z)^2 - (S^x)^2 - (S^y)^2]. \tag{8}$$

As discussed in the Supplementary material of Ref. [19], the biquadratic term of the Hamiltonian (3) can be rewritten as

$$(\mathbf{S}_i \cdot \mathbf{S}_{i+1})^2 = \frac{4}{3} - \frac{1}{2}\sum_{a=1}^{3} T_i^a T_{i+1}^a + \frac{1}{2}\sum_{a=4}^{8} T_i^a T_{i+1}^a. \tag{9}$$

Therefore, the Hamiltonian (3) can be rewritten as

$$\mathcal{H} = \cos\theta \sum_{i=1}^{N_s} \mathbf{S}_i \cdot \mathbf{S}_{i+1} + \sin\theta \sum_{i=1}^{N_s} (\mathbf{S}_i \cdot \mathbf{S}_{i+1})^2 \tag{10}$$

$$= \frac{4}{3}\sin\theta + \left(\cos\theta - \frac{1}{2}\sin\theta\right) \sum_{a=1}^{3} T_i^a T_{i+1}^a + \frac{1}{2}\sin\theta \sum_{a=4}^{8} T_i^a T_{i+1}^a, \tag{11}$$

so at $\theta = \pi/4$ it becomes

$$H(\theta = \pi/4) = \sum_{i=1}^{N_s} \mathbf{S}_i \cdot \mathbf{S}_{i+1} + \sum_{i=1}^{N_s} (\mathbf{S}_i \cdot \mathbf{S}_{i+1})^2 = \frac{4}{3} + \frac{1}{2} \sum_{i=1}^{N_s} \sum_{a=1}^{8} T_i^a T_{i+1}^a, \tag{12}$$

which is equivalent to the antiferromagnetic SU(3) Heisenberg chain. At $\theta = 5\pi/4$ the model becomes SU(3) symmetric again, with a highly degenerate ground state (as discussed in Ref. [20]). The two SU(3) symmetric Hamiltonians are connected as $H(\theta = 5\pi/4) = -H(\theta = \pi/4)$. In these cases, the three $s = 1$ basis states on every site become the three SU(3) spin states.

For all other $\theta \notin \{\pi/4, 5\pi/4\}$, the model has no SU(3) symmetry, and the quadrupolar operators of Eqs. (8) have different weights is the Hamiltonian (3) as the spin operators S^x, S^y, and S^z. Consequently, the correlation functions of the spin and quadrupolar operators are different $\langle \mathrm{GS}|S_i^a S_j^a|\mathrm{GS}\rangle \neq \langle \mathrm{GS}|Q_i^b Q_j^b|\mathrm{GS}\rangle$ in the ground state $|\mathrm{GS}\rangle$ of the Hamiltonian (3), unlike in the SU(3) model.

According to Ref. [21], for $-\pi/4 < \theta < \pi/4$ the model becomes gapped, we enter the Haldane phase, where the ground state is a quantum spin liquid with topological order [22, 23]. For $\pi/4 \leq \theta \leq \pi/2$ the model remains gapless, with dominant $k = \pm 2\pi/3$ spin quadrupolar correlations. Around the other SU(3) symmetric point (at $\theta = 5\pi/4$), for $\pi < \theta < 5\pi/4$ the model becomes ferromagnetic, and for $5\pi/4 < \theta < 7\pi/4$ the ground state is dimerized.

References

[1] O. V. Gamayun, V. P. Ostroukh, N. V. Gnezdilov, Adagideli, and C. W. J. Beenakker, "Valley-momentum locking in a graphene superlattice with y-shaped kekulé bond texture," *New Journal of Physics*, vol. 20, no. 2, p. 023016, feb 2018. [Online]. Available: https://dx.doi.org/10.1088/1367-2630/aaa7e5

[2] Z. Zhu and S. R. White, "Spin liquid phase of the $s = \frac{1}{2}$ $J_1 - J_2$ heisenberg model on the triangular lattice," *Phys. Rev. B*, vol. 92, p. 041105, Jul 2015. [Online]. Available: https://link.aps.org/doi/10.1103/PhysRevB.92.041105

[3] C. A. Gallegos, S. Jiang, S. R. White, and A. L. Chernyshev, "Phase diagram of the easy-axis triangular-lattice $J_1{-}J_2$ model," *Phys. Rev. Lett.*, vol. 134, p. 196702, May 2025. [Online]. Available: https://link.aps.org/doi/10.1103/PhysRevLett.134.196702

[4] Y. Iqbal, W.-J. Hu, R. Thomale, D. Poilblanc, and F. Becca, "Spin liquid nature in the heisenberg $J_1 - J_2$ triangular antiferromagnet," *Phys. Rev. B*, vol. 93, p. 144411, Apr 2016. [Online]. Available: https://link.aps.org/doi/10.1103/PhysRevB.93.144411

[5] F. Ferrari and F. Becca, "Dynamical structure factor of the $J_1 - J_2$ heisenberg model on the triangular lattice: Magnons, spinons, and gauge fields," *Phys. Rev. X*, vol. 9, p. 031026, Aug 2019. [Online]. Available: https://link.aps.org/doi/10.1103/PhysRevX.9.031026

[6] H. Jia, B. Ma, Z. D. Wang, and G. Chen, "Quantum spin supersolid as a precursory dirac spin liquid in a triangular lattice antiferromagnet," *Phys. Rev. Res.*, vol. 6, p. 033031, Jul 2024. [Online]. Available: https://link.aps.org/doi/10.1103/PhysRevResearch.6.033031

[7] U. F. P. Seifert, J. Willsher, M. Drescher, F. Pollmann, and J. Knolle, "Spin-peierls instability of the u(1) dirac spin liquid," *Nature Communications*, vol. 15, p. 7110, Aug 2024. [Online]. Available: https://doi.org/10.1038/s41467-024-51367-w

[8] B. Huang, W. Choi, Y. B. Kim, and Y.-M. Lu, "Classification and properties of quantum spin liquids on the hyperhoneycomb lattice," *Phys. Rev. B*, vol. 97, p. 195141, May 2018. [Online]. Available: https://link.aps.org/doi/10.1103/PhysRevB.97.195141

[9] Y. X. Zhao, Y. Lu, and S. A. Yang, "Topological second-order spin-3/2 liquids with hinge fermi arcs," 2020. [Online]. Available: https://arxiv.org/abs/2005.14500

[10] C. Liu, G. B. Halász, and L. Balents, "Symmetric u(1) and F_2 spin liquids on the pyrochlore lattice," *Phys. Rev. B*, vol. 104, p. 054401, Aug 2021. [Online]. Available: https://link.aps.org/doi/10.1103/PhysRevB.104.054401

[11] J. C. Luaces, M. F. López, A. G. Blázquez, J. Bravo-Abad, and J. Merino, "Topological strongly correlated phases in orthorhombic diamond lattice compounds," *Phys. Rev. B*, vol. 111, p. 165133, Apr 2025. [Online]. Available: https://link.aps.org/doi/10.1103/PhysRevB.111.165133

[12] S. Florens and A. Georges, "Quantum impurity solvers using a slave rotor representation," *Phys. Rev. B*, vol. 66, p. 165111, Oct 2002. [Online]. Available: https://link.aps.org/doi/10.1103/PhysRevB.66.165111

[13] J. N. Nelson, J. P. Ruf, Y. Lee, C. Zeledon, J. K. Kawasaki, S. Moser, C. Jozwiak, E. Rotenberg, A. Bostwick, D. G. Schlom, K. M. Shen, and L. Moreschini, "Dirac nodal lines protected against spin-orbit interaction in iro_2," *Phys. Rev. Mater.*, vol. 3, p. 064205, Jun 2019. [Online]. Available: https://link.aps.org/doi/10.1103/PhysRevMaterials.3.064205

[14] Q. Wang, A. de la Torre, J. A. Rodriguez-Rivera, A. A. Podlesnyak, W. Tian, A. A. Aczel, M. Matsuda, P. J. Ryan, J.-W. Kim, J. G. Rau, and K. W. Plumb, "Pulling order back from the brink of disorder: Observation of a nodal-line spin liquid and fluctuation stabilized order in k_2ircl_6," *Phys. Rev. X*, vol. 15, p. 021021, Apr 2025. [Online]. Available: https://link.aps.org/doi/10.1103/PhysRevX.15.021021

[15] M. Hermele, V. Gurarie, and A. M. Rey, "Mott insulators of ultracold fermionic alkaline earth atoms: Underconstrained magnetism and chiral spin liquid," *Phys. Rev. Lett.*, vol. 103, p. 135301, Sep 2009. [Online]. Available: https://link.aps.org/doi/10.1103/PhysRevLett.103.135301

[16] M. Hermele and V. Gurarie, "Topological liquids and valence cluster states in two-dimensional su(n) magnets," *Phys. Rev. B*, vol. 84, p. 174441, Nov 2011. [Online]. Available: https://link.aps.org/doi/10.1103/PhysRevB.84.174441

[17] X.-P. Yao, Y. Gao, and G. Chen, "Topological chiral spin liquids and competing states in triangular lattice SU(n) mott insulators," *Phys. Rev. Res.*, vol. 3, p. 023138, May 2021. [Online]. Available: https://link.aps.org/doi/10.1103/PhysRevResearch.3.023138

[18] H.-K. Jin, J.-J. Miao, and Y. Zhou, "Hidden su(2) symmetries, the symmetry hierarchy, and the emergent eightfold way in spin-1 quantum magnets," *Phys. Rev. B*, vol. 100, p. 085101, Aug 2019. [Online]. Available: https://link.aps.org/doi/10.1103/PhysRevB.100.085101

[19] V. L. Quito, J. A. Hoyos, and E. Miranda, "Emergent su(3) symmetry in random spin-1 chains," *Phys. Rev. Lett.*, vol. 115, p. 167201, Oct 2015. [Online]. Available: https://link.aps.org/doi/10.1103/PhysRevLett.115.167201

[20] C. D. Batista, G. Ortiz, and J. E. Gubernatis, "Unveiling order behind complexity: Coexistence of ferromagnetism and bose-einstein condensation," *Phys. Rev. B*, vol. 65, p. 180402, Apr 2002. [Online]. Available: https://link.aps.org/doi/10.1103/PhysRevB.65.180402

[21] A. Läuchli, G. Schmid, and S. Trebst, "Spin nematics correlations in bilinear-biquadratic $s = 1$ spin chains," *Phys. Rev. B*, vol. 74, p. 144426, Oct 2006. [Online]. Available: https://link.aps.org/doi/10.1103/PhysRevB.74.144426

[22] F. Haldane, "Continuum dynamics of the 1-d heisenberg antiferromagnet: Identification with the o(3) nonlinear sigma model," *Physics Letters A*, vol. 93, no. 9, pp. 464–468, 1983. [Online]. Available: https://www.sciencedirect.com/science/article/pii/037596018390631X

[23] F. D. M. Haldane, "Nonlinear field theory of large-spin heisenberg antiferromagnets: Semiclassically quantized solitons of the one-dimensional easy-axis néel state," *Phys. Rev. Lett.*, vol. 50, pp. 1153–1156, Apr 1983. [Online]. Available: https://link.aps.org/doi/10.1103/PhysRevLett.50.1153